SCIENCE CHINA
Physics, Mechanics & Astronomy

• Article •

October 2015 Vol. 58 No. 10: 107801
doi: 10.1007/s11433-015-5717-0

CVD synthesis of nitrogen-doped graphene using urea†

ZHANG CanKun, LIN WeiYi, ZHAO ZhiJuan, ZHUANG PingPing, ZHAN LinJie, ZHOU YingHui & CAI WeiWei*

Department of Physics, Laboratory of Nanoscale Condense Matter Physics and State Key Laboratory of Physical Chemistry of Solid Surfaces, Xiamen University, Xiamen 361005, China

Received June 10, 2015; accepted June 29, 2015

This work provides an effective low-cost synthesis and in-depth mechanistic study of high quality large-area nitrogen-doped graphene (NG) films. These films were synthesized using urea as nitrogen source and methane as carbon source, and were characterized by scanning electron microscopy (SEM), Raman spectroscopy and X-ray photoelectron spectroscopy (XPS). The N doping level was determined to be 3.72 at.%, and N atoms were suggested to mainly incorporated in a pyrrolic N configuration. All distinct Raman peaks display a shift due to the nitrogen-doping and compressive strain. The increase in urea concentration broadens the *D* and 2*D* peak's Full Width at Half Maximum (FWHM), due to the decrease of mean free path of phonons. The N-doped graphene exhibited an n-type doping behavior with a considerably high carrier mobility of about 74.1 $cm^2/(V\ s)$, confirmed by electrical transport measurements.

nitrogen-doped graphene, chemical vapor deposition, Raman spectroscopy, X-ray photoemission spectroscopy

PACS number(s): 81.15.Gh, 78.30.-j, 33.60.Fy

Citation: Zhang C K, Lin W Y, Zhao Z J, et al. CVD synthesis of nitrogen-doped graphene using urea. Sci China-Phys Mech Astron, 2015, 58: 107801, doi: 10.1007/s11433-015-5717-0

1 Introduction

Graphene is an atomic-scale honeycomb crystal lattice consisting of sp^2 carbon atoms. It has received considerable interest since its first isolation in 2004 [1], due to its extraordinary electrical properties [2], such as high charge carrier mobility [3], high thermal conductivity [2,4–9], room-temperature quantum Hall effect [10], thus making graphene a promising material for future nanoelectronics [4]. For the application of graphene in nanoelectronics, that requires rapid on/off switching, it is important to be able to modulate its electronic properties without affecting its high mobility [11]. Surface depositing [12] and heteroatoms doping are ways to control the electronic properties of semiconductor. However, heteroatoms doping can also be employed in graphene to tailor its electronic band structure [13,14]. Among all available heteroatom dopants, nitrogen has attracted considerable attention due to its similar atomic radii to that of carbon atom and n-type electronic behavior of nitrogen doped grapheme [15,16]. Several approaches are used to synthesize N-doped graphene, such as chemical vapor deposition (CVD) [15,17–22], arc discharge [23], graphene oxide reaction [24–27], N plasma treatment [28–30], solvothermal synthesis [31], post thermal annealing of graphene with NH_3 [27,32]. The CVD technique is chosen due to its simplicity, low-cost, and reproducibility in fabrication of large-scale, uniform N-doped graphene films [33].

In this work, we synthesized continuous single layered N-doped graphene (NG) on Cu substrates by the CVD technique using urea ($CO(NH_2)_2$) as the N dopant, methane (CH_4) as a carbon source and hydrogen (H_2) as catalyst/carrier gas. Urea is inexpensive, readily available and has high nitrogen content. The resultant NG films exhibit

*Corresponding author (email: wwcai@xmu.edu.cn)
†Recommended by ZHAO Hong (Associate Editor)

comparable properties to that of reported NG films [17], with the N content of the NG film at 3.72 at.%. The Dirac point, mobility are –52.9 V, and 74.1 cm^2/V s respectively.

2 Experimental

2.1 Synthesis of N-doped grapheme

The N-doped graphene (NG) was grown on the interior surfaces of 25 μm copper foil (Alfa Aesar, Stock no. 46365, 99.8%) by CVD using a gas mixture of H_2, CH_4 and $CO(NH_2)_2$. Copper foil was etched in $(NH_4)_2S_2O_8/H_2O$–3 g/100 mL) solution, rinsed/dried and folded into a square pocket [3]. The pocket was then placed into another bigger copper pocket for protection against erosion, and was loaded into the 1 inch quartz tube inside a horizontal furnace. A ceramic dish containing 100 mg of urea was placed into the same tube upstream, about 15 cm away from the heater zone. The heating belt was around the tube where the urea charge was located, as illustrated in Figure 1(a). After that, the system was pumped to 7.5 mTorr. The furnace temperature was then ramped to 1000°C and the temperature maintained for 20 min with the flow rate of 10 sccm H_2 for annealing. During the growth process, heating belt was heated to 60°C to generate urea vapor; CH_4 and H_2 were introduced into the chamber, both with a fixed flow rate of 10 sccm. The process pressure was maintained at 398 mTorr. For comparison, the pristine graphene (PG) was synthesized by the same process without introducing any nitrogen source. A recent paper states the use of urea as nitrogen source and polystyrene as carbon source to synthesize N-doped grapheme [34]. Our method is superior because all components can be mix homogenously and is lower cost.

2.2 Transfer of NG and PG

The graphene/Cu substrate was spin-coated with PMMA (MW 350000; 46 mg/mL in chlorobenzene). After etching of the underlying Cu foil using copper etchant $(NH_4)_2S_2O_8/H_2O$ (3 g/100 mL), the free-standing PMMA/graphene membrane was washed with the DI water for 20 min. Then it was transferred onto a silicon substrate with 300 nm SiO_2, followed by heating at 50°C for 20 min. Finally, the PMMA was removed using acetone. After a final rinse with ethanol, graphene film on SiO_2/Si substrate was ready for further investigations.

2.3 Characterizations of NG and PG

The NG samples were characterized by scanning electron microscopy (SEM) (ZEISS SIGMA), atomic force microscopy (AFM) (SPA 400), Raman spectroscopy (WiTec Alfa 300, with 488 nm laser), X-ray photoelectron spectroscopy (XPS) (PHI Quantum-2000). Device fabrication and electrical measurements of the PG and NG on SiO_2/Si were used for fabrication of back-gated field-effect transistor (FETs). Copper electrodes were plated onto the graphene films; the graphene films act as the conducting channel between the sources and drain electrodes. The channel length (L) and width (W) were both about 1 cm. The electrical properties were measured in air at room temperature.

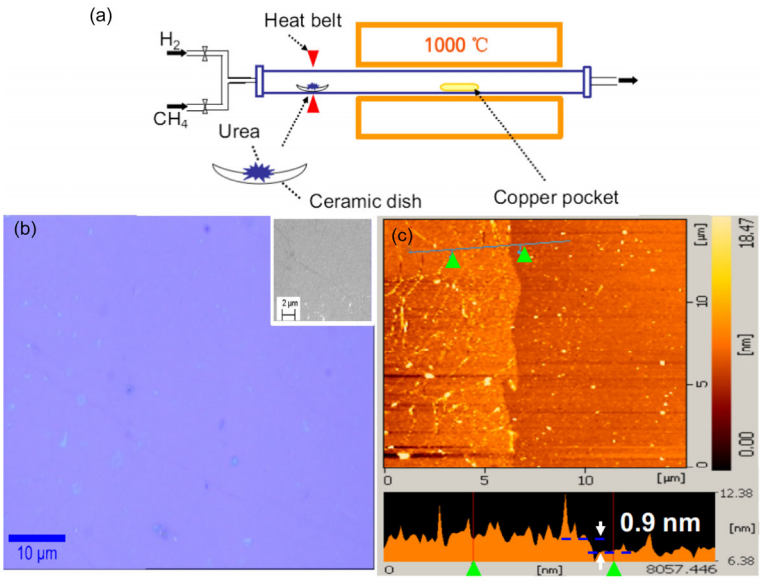

Figure 1 (Color online) (a) Illustrative picture of system for the synthesis of NG film on Cu foil by using urea as the nitrogen source; (b) optical image of a single layer NG transferred onto SiO_2/Si substrate. Inset is SEM image of NG transferred onto SiO_2/Si substrate; (c) AFM image of NG at the edge of NG transferred onto SiO_2/Si substrate and with an average thickness of 0.9 nm.

3 Results and discussion

The system for the synthesis of NG film on Cu foil with urea as the nitrogen source is illustrated in Figure 1(a), while the detailed growth procedure is presented in the experimental section. Basically, in a low-pressure CVD reactor, the urea powder sublimated at 60°C upstream and transported by H_2 and CH_4 gas to the copper foil to decompose and react to form NG at 1000°C. After being transferred from the copper foil onto a SiO_2/Si substrate, the NG film was displayed as a large-area, uniform and continuous film from the optical (Figure 1(b)) and SEM (inset Figure 1(b)) images. The thickness of the NG film was determined by AFM. As shown in Figure 1(c), the average thickness of NG was 0.9 nm.

Raman spectra of pristine graphene (black curve) and nitrogen-doped graphene (red curve) on 300 nm SiO_2/Si substrate are exhibited in Figure 2. Two conspicuous peaks in PG are the *G* band (1571 cm^{-1}) and the 2*D* band (2681 cm^{-1}), characteristic features for a single layer graphene [35]. In addition, a weak Raman peak at 1350 cm^{-1} has been assigned to *D* band, activated by defects via an intervalley double-resonance Raman process [36]. And the intensity ratio of *D* band to *G* band (I_D/I_G) has been used to evaluate the defect density in grapheme [36,37]. The tiny intensity ratio ($I_D/I_G \approx 0$) demonstrates that the pristine graphene nearly has almost no defects. In contrast, the N-doped graphene displays a much higher intensity of the *D* band at 1356 cm^{-1}. The intensity ratio (I_D/I_G) is about 2.19, due to the structure defects induced by nitrogen doping [16]. An extra peak (*D*′; 1630 cm^{-1}) located on the shoulder of *G* peak is also observed for NG. It originates from the intravalley double resonance scattering process, in which the defects provide the missing momentum in order to satisfy the resonant process [38]. Compared with that of PG, the I_{2D}/I_G ratio decreases, because the 2*D* peak is sensitive to lattice defects and doping in grapheme [39,40]. *G* band (1593.71 cm^{-1}) and 2*D* band (2696.80 cm^{-1}) of the NG show upshifts of about 6 and 15 cm^{-1}, respectively. We also synthesized graphenes with different dopant concentration and study how their Raman spectra changed with the dopant concentration (I_D/I_G) (Figure 3).

As shown in Figures 3(a)–(d), all conspicuous peaks shift to higher frequencies with the increase of the dopant concentration (I_D/I_G). Electron doping [41,42] and compressive strain [43] also contributed to such shift, as explained previously [40]. The larger dopant concentration, the more electrons doping, and the more distortion of the lattice all lead to the more blue shift of Raman peaks. Figures 3(e) and (f) show that $I_{D'}/I_G$ increases, whereas I_{2D}/I_G decreases with the increase of I_D/I_G, which is contributed with combination of lattice defects and charge carrier doping [39,40,44]. By using the ratio $I_D/I_{D'}$, we can probe the nature of defects.

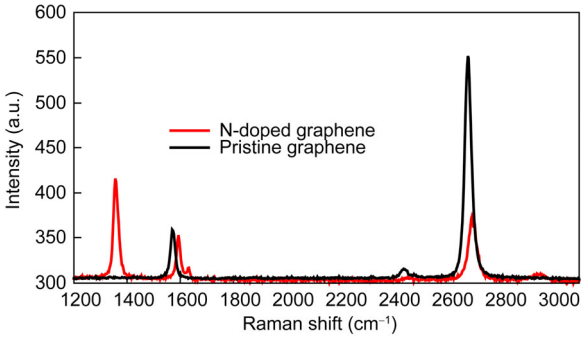

Figure 2 (Color online) Raman spectra of PG (black) and NG (red) on 300 nm SiO_2/Si substrate.

According to the previous reports [40,45], $I_D/I_{D'}$ is ~13 for sp^3-defects, ~7 for vacancy-like defects, and ~3.5 for domain boundaries. The $I_D/I_{D'}$ of NG is about ~1.20, which is close to the 4 value of boundary defects. Figures 3(g) and (h) show the FWHM (Full Width at Half Maximum) of *D* and *2D* peaks, which is strongly dependent on the phonon-defect scattering rate, increasing almost linearly with the increase of I_D/I_G. Our previous work has reported that the point-defect can decrease the phonon lifetime, and consequently decrease the mean free path of phonon and broaden the FWHM of *2D* peak [46].

XPS is applied to study the N content and bonding configurations of N-doped graphene transferred on 300 nm SiO_2/Si substrate. The Nitrogen content of our sample is 3.72 at.%, which is determined by the ratio of peak intensity between N1s and C1s. Figure 4 shows high-resolution XPS C1s spectrum (a) and N1s spectrum (b). In Figure 4(a), the C1s spectrum can be decomposed into three component peaks, with their maxima at binding energy of 284.6, 285.2, and 286.0 eV, respectively. The main peak at 284.6 eV is assigned to sp^2 hybridized C atoms in graphene. The other two peaks at 285.2 and 286.0 eV represent the binding energy of N atoms connected with sp^2 C and sp^3 C atoms due to the substitution of the N atoms and defects in the grapheme [15]. The N1s peak also has three components. The peaks at 399.5 and 400.0 eV correspond to "pyridinic" N and "pyrrolic" N, respectively. They refer to the N atoms which located in a π conjugated system and contribute to the system with one or two p-electrons, respectively [15]. In the graphitic N, located at 401.3 eV, N replaces the carbon atom within the graphene layer and bonds to three carbon atoms. Among the three bonding configuration, the pyrrolic N is the main structure.

Electrical properties measurements of the NG were performed in air at room temperature to reveal the doping effect and carrier mobility. Back-gated field-effect transistors (FETs) based on PG and NG were fabricated on 300 nm SiO_2/Si substrates with copper metal source/drain. Figure 5 displays the typical transfer characteristics of PG and NG FETs at fixed drain-source voltage (V_{ds}=1 V). The back-gate scanning voltage (V_{gs}) scans from −100 to 100 V.

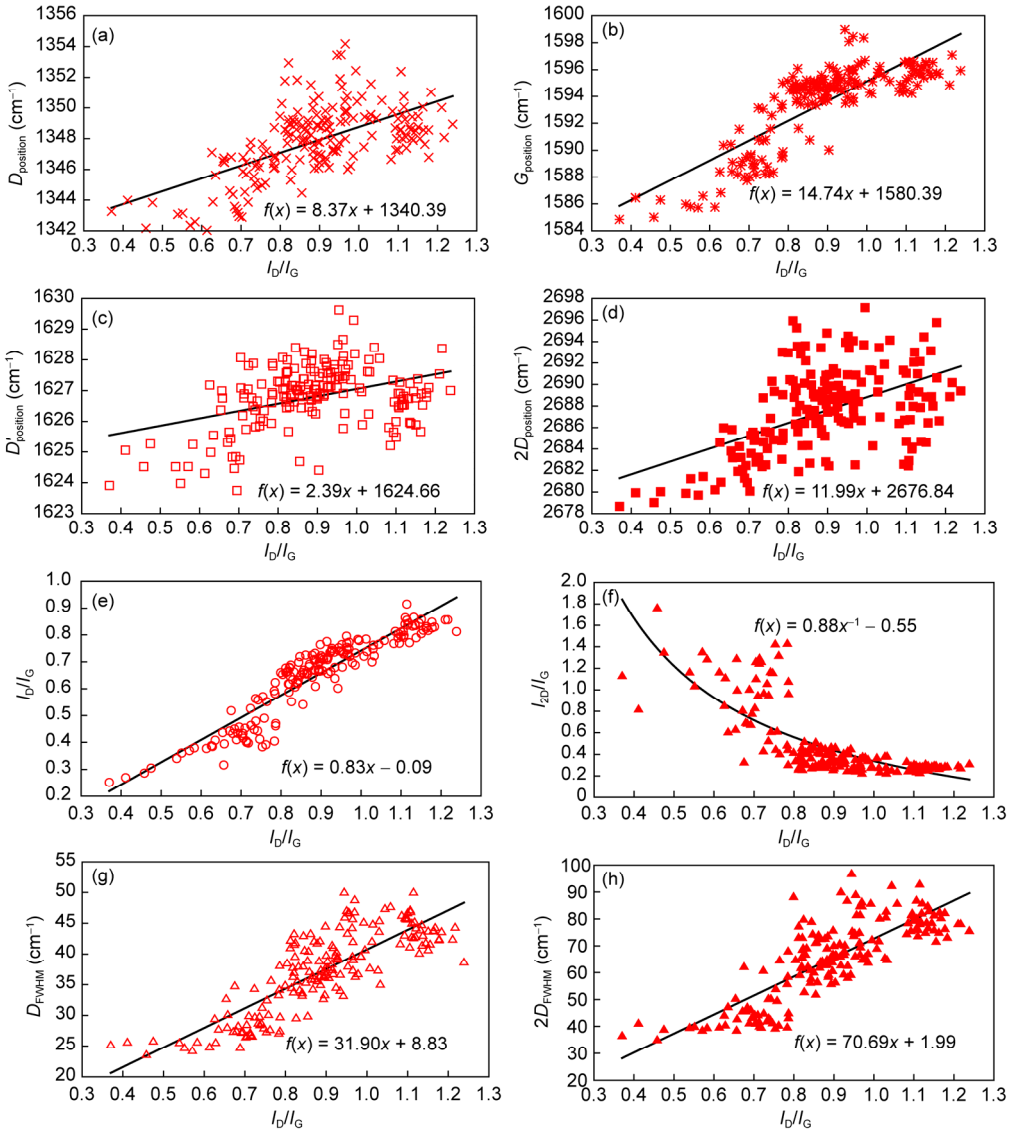

Figure 3 (Color online) Evolution of Raman peaks position of D (a), G (b), D' (c), 2D (d), intensity (D') (e) and 2D (f)) and FWHM (D (g) and 2D (h)).

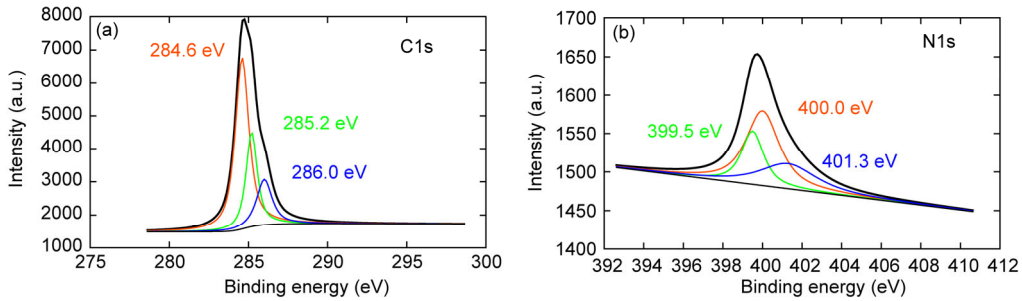

Figure 4 (Color online) High-resolution XPS C1s (a) and N1s (b) spectrum of NG.

The curve of drain current versus gate voltage in Figure 5 reveals a typical n-type conductive behavior of the NG device, with the Dirac point at about −52.9 V. In contrast, the PG device fabricated and measured using the same procedure shows the Dirac point at about 3.31 V, because the residual organics and O_2 etc. are absorbed on the surface of PG, which makes the PG device p-typed. The mobility can be calculated using the equation, where C_0 is the back-gate capacitance with the value of 11.52 nF/cm^{-2}. The electron and hole mobility of NG are calculated to be 17.3 and

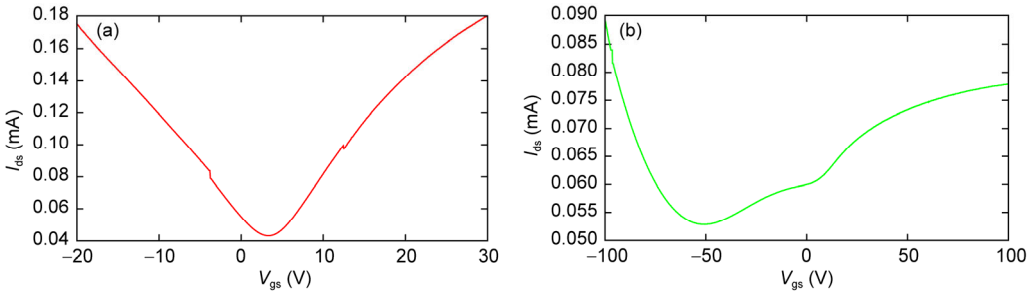

Figure 5 (Color online) Transport properties in pristine (a) and nitrogen-doped (b) graphene devices.

74.1 cm^2/V s, respectively. The hole mobility is comparable to that the previous work 53–73 [47] and 74 cm^{-2}/V s [22]. Although the measurement was carried out in air, the Dirac point at −52.9 V is much larger than that measured in vacuum [17,48] and others in air condition [22,47]. It indicates that NG synthesized by our method has a rich doping content 3.72 at.% and maintains a higher carrier mobility, 74.1 cm^2/V s.

4 Conclusion

We have successfully synthesized continuous, uniform and single layer large area N-doped graphene via CVD method, where urea was used as the N source and methane as the C source. We performed SEM, Raman spectroscopy and X-ray photoelectron spectroscopy (XPS) to characterize the NG. Nitrogen atoms were doped into graphene with N content at 3.72 at.%, verified by Raman and XPS spectroscopy. The configuration was mainly pyrrolic N structure. The electrical studies showed that NG device was typical n-typed in air with Dirac point at −52.9 V and the hole mobility of 74.1 cm^2/V s, which was comparable to that of previous reported NG devices.

This work was supported by the National Natural Science Foundation of China (Grant Nos. 91123009, 10975115), and the Natural Science Foundation of Fujian Province of China (Grant No. 2012J06002).

1 Novoselov K S. Electric field effect in atomically thin carbon films. Science, 2004, 306: 666–669
2 Geim A K. Graphene: Status and prospects. Science, 2009, 324: 1530–1534
3 Li X, Cai W, An J, et al. Large-area synthesis of high-quality and uniform graphene films on copper foils. Science, 2009, 324: 1312–1314
4 Geim A K, Novoselov K S. The rise of graphene. Nat Mater, 2007, 6: 183–191
5 Balandin A A, Ghosh S, Bao W, et al. Superior thermal conductivity of single-layer graphene. Nano Lett, 2008, 8: 902–907
6 Balandin A A. Thermal properties of graphene and nanostructured carbon materials. Nat Mater, 2011, 10: 569–581
7 Chen S S, Wu Q Z, Mishra C, et al. Thermal conductivity of isotopically modified graphene. Nat Mater, 2012, 11: 203–207
8 Nika D L, Balandin A A. Two-dimensional phonon transport in graphene. J Phys Condens Matter, 2012, 24: 233203
9 Chen S D, Zhang Y, Wang J, et al. Connection between heat diffusion and heat conduction in one-dimensional systems. Sci China-Phys Mech Astron, 2013, 56: 1466–1471
10 Novoselov K S, Jiang Z, Zhang Y, et al. Room-temperature quantum hall effect in graphene. Science, 2007, 315: 1379–1379
11 Zhan D, Yan J, Lai L, et al. Engineering the electronic structure of graphene. Adv Mater, 2012, 24: 4055–4069
12 Hou Y X, Geng X M, Li Y Z, et al. Electrical and Raman properties of p-type and n-type modified graphene by inorganic quantum dot and organic molecule modification. Sci China-Phys Mech Astron, 2011, 54: 416–419
13 Deifallah M, McMillan P F, Corà F. Electronic and structural properties of two-dimensional carbon nitride graphenes. J Phys Chem C, 2008, 112: 5447–5453
14 Martins T, Miwa R, da Silva A, et al. Electronic and transport properties of boron-doped graphene nanoribbons. Phys Rev Lett, 2007, 98: 196803
15 Wei D C, Liu Y Q, Wang Y, et al. Synthesis of N-doped graphene by chemical vapor deposition and its electrical properties. Nano Lett, 2009, 9: 1752–1758
16 Wang X R, Li X L, Zhang L, et al. N-doping of graphene through electrothermal reactions with ammonia. Science, 2009, 324: 768–771
17 Sun Z, Yan Z, Yao J, et al. Growth of graphene from solid carbon sources. Nature, 2010, 468: 549–552
18 Zhao L Y, He R, Rim K T, et al. Visualizing individual nitrogen dopants in monolayer graphene. Science, 2011, 333: 999–1003
19 Ito Y, Christodoulou C, Nardi M V, et al. Chemical vapor deposition of N-doped graphene and carbon films: The role of precursors and gas phase. Acs Nano, 2014, 8: 3337–3346
20 Kato T, Hatakeyama R. Direct growth of doping-density-controlled hexagonal graphene on SiO_2 substrate by rapid-heating plasma CVD. Acs Nano, 2012, 6: 8508–8515
21 Terasawa T, Saiki K. Synthesis of nitrogen-doped graphene by plasma-enhanced chemical vapor deposition. Jpn J Appl Phys, 2012, 51: 924–941
22 Wang Z, Li P, Chen Y, et al. Synthesis of nitrogen-doped graphene using sole solid source by chemical vapour deposition. J Mater Chem C, 2014, doi: 10.1039/C4TC00924J
23 Panchokarla L S, Subrahmanyam K S, Saha S K, et al. Synthesis, structure, and properties of boron- and nitrogen-doped graphene. Adv Mater, 2009, 21: 4726–4730
24 Sheng Z H, Shao L, Chen J J, et al. Catalyst-free synthesis of nitrogen-doped graphene via thermal annealing graphite oxide with melamine and its excellent electrocatalysis. Acs Nano, 2011, 5: 4350–4358
25 Long D H, Li W, Ling L C, et al. Preparation of nitrogen-doped graphene sheets by a combined chemical and hydrothermal reduction of graphene oxide. Langmuir, 2010, 26: 16096–16102

26 Wang H B, Zhang C J, Liu Z H, et al. Nitrogen-doped graphene nanosheets with excellent lithium storage properties. J Mater Chem, 2011, 21: 5430–5434

27 Sun L, Wang L, Tian C G, et al. Nitrogen-doped graphene with high nitrogen level via a one-step hydrothermal reaction of graphene oxide with urea for superior capacitive energy storage. Rsc Adv, 2012, 2: 4498–4506

28 Wang Y, Shao Y Y, Matson D W, et al. Nitrogen-doped graphene and its application in electrochemical biosensing. Acs Nano, 2010, 4: 1790–1798

29 Shao Y Y, Zhang S, Engelhard M H, et al. Nitrogen-doped graphene and its electrochemical applications. J Mater Chem, 2010, 20: 7491–7496

30 Guo B, Liu Q, Chen E, et al. Controllable N-doping of graphene. Nano Lett, 2010, 10: 4975–4980

31 Deng D H, Pan X L, Yu L A, et al. Toward N-doped graphene via solvothermal synthesis. Chem Mater, 2011, 23: 1188–1193

32 Geng D S, Yang S L, Zhang Y, et al. Nitrogen doping effects on the structure of graphene. Appl Surf Sci, 2011, 257: 9193–9198

33 Li J Y, Ren Z Y, Zhou Y X, et al. Scalable synthesis of pyrrolic N-doped graphene by atmospheric pressure chemical vapor deposition and its terahertz response. Carbon, 2013, 62: 330–336

34 Wu T R, Shen H L, Sun L, et al. Nitrogen and boron doped monolayer graphene by chemical vapor deposition using polystyrene, urea and boric acid. New J Chem, 2012, 36: 1385–1391

35 Ferrari A C, Meyer J C, Scardaci V, et al. Raman spectrum of graphene and graphene layers. Phys Rev Lett, 2006, 97: 187401

36 Luo Z Q, Lim S H, Tian Z Q, et al. Pyridinic N doped graphene: Synthesis, electronic structure, and electrocatalytic property. J Mater Chem, 2011, 21: 8038–8044

37 Pimenta M A, Dresselhaus G, Dresselhaus M S, et al. Studying disorder in graphite-based systems by Raman spectroscopy. Phys Chem Chem Phys, 2007, 9: 1276–1291

38 Malard L M, Pimenta M A, Dresselhaus G, et al. Raman spectroscopy in graphene. Phys Rep, 2009, 473: 51–87

39 Venezuela P, Lazzeri M, Mauri F. Theory of double-resonant Raman spectra in graphene: Intensity and line shape of defect-induced and two-phonon bands. Phys Rev B, 2011, 84: 945–949

40 Zafar Z, Ni Z H, Wu X, et al. Evolution of Raman spectra in nitrogen doped graphene. Carbon, 2013, 61: 57–62

41 Pisana S, Lazzeri M, Casiraghi C, et al. Breakdown of the adiabatic Born-Oppenheimer approximation in graphene. Nat Mater, 2007, 6: 198–201

42 Das A, Pisana S, Chakraborty B, et al. Monitoring dopants by Raman scattering in an electrochemically top-gated graphene transistor. Nat Nanotechnol, 2008, 3: 210–215

43 Ni Z H, Yu T, Lu Y H, et al. Uniaxial strain on graphene: Raman spectroscopy study and band-gap opening. ACS Nano, 2008, 2: 2301–2305

44 Ni Z H, Yu T, Luo Z Q, et al. Probing charged impurities in suspended graphene using Raman spectroscopy. ACS Nano, 2009, 3: 569–574

45 Eckmann A, Felten A, Mishchenko A, et al. Probing the nature of defects in graphene by Raman spectroscopy. Nano Lett, 2012, 12: 3925–3930

46 Zhang C K, Li Q Y, Tian B, et al. Isotope effect of the phonons mean free path in graphene by micro-Raman measurement. Sci China-Phys Mech Astron, 2014, 57: 1817–1821

47 Xue Y, Wu B, Jiang L, et al. Low temperature growth of highly nitrogen-doped single crystal graphene arrays by chemical vapor deposition. J Am Chem Soc, 2012, 134: 11060–11063

48 Jin Z, Yao J, Kittrell C, et al. Large-scale growth and characterizations of nitrogen-doped monolayer graphene sheets. Acs Nano, 2011, 5: 4112–4117